Structure and ionic conduction in CuI: diffuse neutron scattering and RMC modelling

A Chahid and R L McGreevy

Studsvik Neutron Research Laboratory, S-611 82 Nykoping, Sweden

Abstract. Total structure factors (Bragg and diffuse scattering) for CuI in γ-, β- and α-phases have been measured by powder neutron diffraction. Reverse Monte Carlo (RMC) modelling of the data has been used to obtain detailed information on the distribution of mobile Cu^+ ions. The RMC results in the γ- and α-phases are in good agreement with molecular dynamics (MD) simulation and Rietveld refinement (RR) of high-resolution (Bragg scattering) powder neutron diffraction data; they confirm that the dominant diffusion pathway is in $\langle 100 \rangle$ directions, directly between tetrahedrally coordinated Cu^+ sites. The octahedral site is not occupied, though there is a very small level of diffusion through this site, along $\langle 111 \rangle$ directions, at the highest temperatures. There are small differences between RMC, MD and RR in the β-phase. In all phases the radial distribution functions obtained from experiment are significantly different from the MD results. It is shown clearly that there is a relationship between the experimental observation of a broad diffuse scattering peak at $Q \sim 1$ Å^{-1} in the structure factor for the β- and α-phases and the existence of a short-distance peak in $g_{CuCu}(r)$ in the RMC models.

1. Introduction

At ambient pressure CuI has three crystallographic phases (see e.g. [1]). Below 642 K it is in the γ-phase where the I^- ions occupy a face centred cubic (fcc) sub-lattice with Cu^+ ions on a similar fcc sub-lattice shifted by $(\frac{1}{4}, \frac{1}{4}, \frac{1}{4})$, forming the zinc-blende structure with space group $F\bar{4}3m$. Between 642 and 680 K it is in the β-phase which has a slightly distorted hexagonal closed packed I^- sub-lattice, similar to wurtzite, with space group $P\bar{3}m1$. Above 680 K it transforms back to an fcc I^- sub-lattice, but four Cu^+ now occupy randomly the eight $(\frac{1}{4}, \frac{1}{4}, \frac{1}{4})$ sites which are tetrahedrally coordinated by I^-; this is the α-phase with space group $Fm\bar{3}m$. Both β- and α-phases have a high ionic (Cu^+) conductivity. There is also evidence of a short-lived rhombohedral structure which can co-exist with the β-phase [1]; this may be considered as a distorted form of the α-phase. α-, β- and γ-phases are illustrated in figure 1; for the β-phase the orthorhombic equivalent cell is shown. In all phases Cu^+ sites are tetrahedrally coordinated to four I^-.

In earlier work we have studied the structure and ionic conductivity in all three phases using molecular dynamics (MD) simulation [2–4], hereafter referred to as MD–JM. The potentials for the simulations were chosen in order to reproduce the experimentally measured diffusion constants [5, 6]. Early diffraction studies observed large thermal vibrations along $\langle 111 \rangle$ [7] and therefore suggested diffusion in this direction. However more recent studies [1] found no Cu^+ occupation of the octahedral $(\frac{1}{2}, \frac{1}{2}, \frac{1}{2})$ site, thus suggesting that $\langle 111 \rangle$ was not the diffusion direction, but were unable to propose an alternative. The MD–JM simulations revealed that the preferred diffusion direction was $\langle 100 \rangle$, despite very large
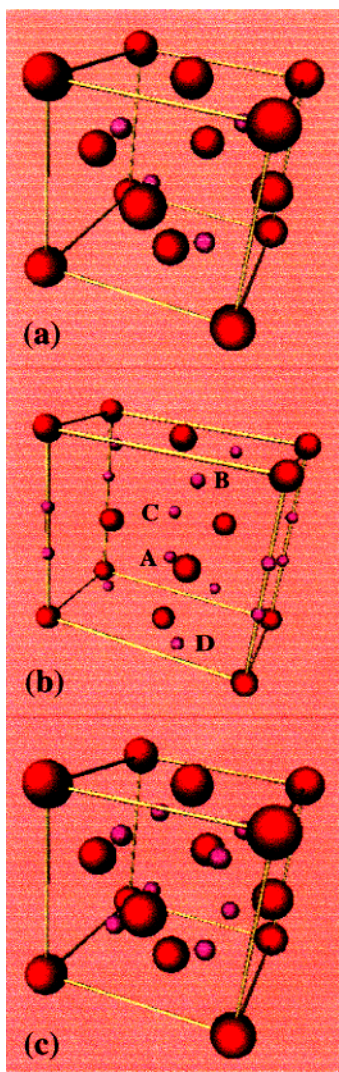
2597

Figure 1. Crystal structures for CuI in the (a) γ-, (b) β- and (c) α-phases. The larger spheres represent I^- sites and the smaller spheres are Cu^+ sites.

thermal vibrations along $\langle 111 \rangle$. However the partial radial distribution functions derived from MD–JM appeared to have first peaks which were rather asymmetric; no evidence of such asymmetry had been found from experimental studies of fast-ion-conducting CuBr [8]. This suggested that the potential used in the MD–JM study may be producing some local structural distortions which are not present in reality. In order to check on this aspect, to further test the validity of the simulations, and also to obtain data which might help in the derivation of improved potentials for further simulations, we have undertaken a diffuse neutron scattering and reverse Monte Carlo (RMC) modelling study of CuI as described in this paper.

In a separate context, it is also interesting to compare the results of the present type of study with those from a more 'conventional' crystallographic approach. Here we measure

total scattering data, that is both Bragg and (energy integrated) diffuse scattering, and analyse them by RMC modelling. Total scattering provides information on the instantaneous correlations of atoms, i.e. a 'snap-shot' picture of the structure. Elastic Bragg scattering alone, typically analysed using Rietveld refinement (RR), provides information on the time average structure. For materials at low temperature with well defined crystal structures and harmonic vibrations these different analyses are effectively the same (i.e. there is very little diffuse scattering), but for CuI at high temperatures where there are large anharmonic vibrations and ionic diffusion the results could be rather different.

2. Experimental details

Diffraction measurements were carried out using the SLAD diffractometer at the Studsvik Neutron Research Laboratory. The incident wavelength was 1.11 Å. A finely powdered sample was contained in a thin-walled vanadium cylinder of diameter 8 mm and measurements were made at 298 and 588 K (γ-phase), 663 K (β-phase) and 698 and 713 K (α-phase). Typically 12 separate scans of 60 minutes were made at each temperature to ensure that the system was in equilibrium. The raw data were corrected for background and container scattering and absorption, self-absorption and inelastic scattering and absolutely normalized to a vanadium standard using the program CORRECT. The resulting structure factors, $F(Q)$, including both Bragg and diffuse scattering, are shown in figure 2. It can clearly be seen that diffuse scattering increases with temperature in the γ-phase, even though the ionic conductivity is still low, but it then increases significantly in the β-phase as the ionic conductivity jumps. It is interesting to note that there is a distinct diffuse scattering peak at low Q, around 1 Å^{-1}, in both β- and α-phases. In the β-phase there is also a Bragg peak in this region. This will be discussed in more detail later.

3. Reverse Monte Carlo modelling

The RMC method and its application to the study of crystalline fast ion conductors has been described in detail elsewhere (e.g. [9]). Here we will only give relevant details. In all cases the initial anion configurations were those corresponding to the perfect crystal structures, with lattice parameters and average atomic positions as determined by Rietveld refinement of neutron diffraction data [1]. These are consistent with the present data.

For the γ- and α-phases models consisted of $8 \times 8 \times 8$ unit cells (4096 ions) in a cubic box of appropriate dimensions with periodic boundary conditions. Initially I$^-$ ions were placed at the cube corners and face centre positions. For the γ-phase Cu$^+$ ions were placed at the 4(c) positions, e.g. $(\frac{1}{4}, \frac{1}{4}, \frac{1}{4})$, $(\frac{1}{4}, \frac{3}{4}, \frac{3}{4})$, $(\frac{3}{4}, \frac{1}{4}, \frac{3}{4})$ and $(\frac{3}{4}, \frac{3}{4}, \frac{1}{4})$ (see figure 1(a)). For the α-phase four Cu$^+$ ions were randomly distributed over all 8(c) $(\frac{1}{4}, \frac{1}{4}, \frac{1}{4})$ type positions (see figure 1(c)).

In the β-phase we have produced configurations using both orthorhombic and hexagonal cells; the results are very similar. Technically the orthorhombic cell is to be preferred since it is possible to produce a configuration with more equal dimensions in all directions. This configuration consisted of $8 \times 8 \times 13$ cells (6656 ions) in a box of dimensions $57.49 \times 59.60 \times 56.16$ Å. I$^-$ ions were placed at $(0, 0, 0)$, $(0, 0.5, 0.5)$, $(0.5, 0.68, 0)$ and $(0.5, 0.176, 0.5)$. Within the average crystal structure four Cu$^+$ ions occupy the eight possible tetrahedral interstices in the I$^-$ sub-lattice (see figure 1(b)); however it has been suggested that there may be correlations between the sites [10]. In order to avoid imposing any such correlation, but also to avoid 'not imposing' it, we have produced one initial
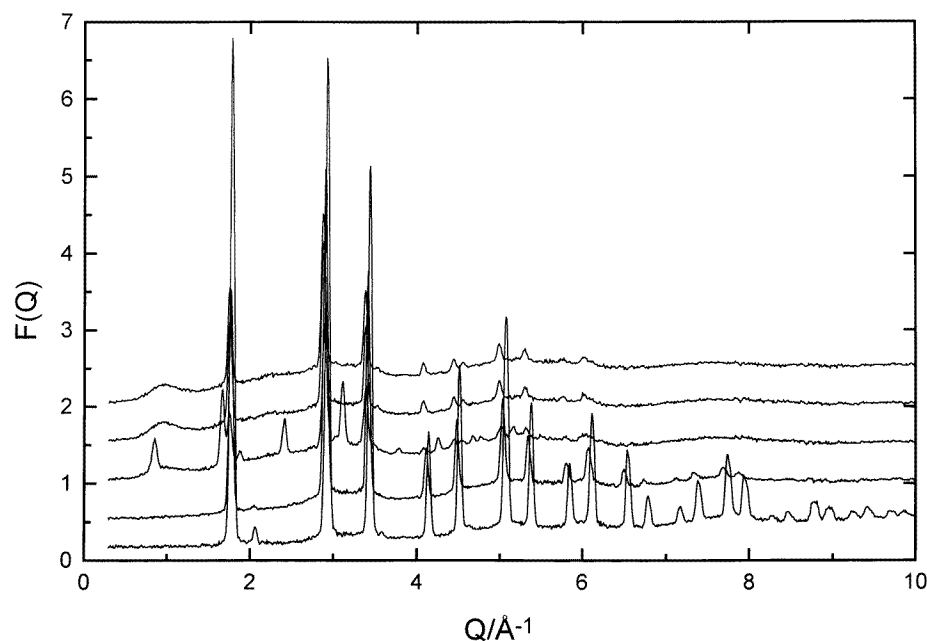
Figure 2. Total structure factors, $F(Q)$, for CuI at, in ascending order, 298 and 588 K in the γ-phase, 663 K in the β-phase and 698 and 713 K in the α-phase. Each set of data is shifted by 0.5 for clarity.

configuration (model β-I) by placing the Cu^+ ions in the four available positions which lie midway between the pairs of tetrahedral sites, that is midway between the sites labelled A and C (or B and D) in figure 1. These positions have triangular threefold Cu–I coordination and have no physical significance, but for this reason do not impose any bias on the initial structure which might influence the final result. We have also produced an initial configuration (model β-II) with Cu^+ ions randomly occupying the tetrahedral positions, but without simultaneous occupation of neighbouring A/C or B/D sites.

Allowed closest approach distances of atoms were initially estimated from the total radial distribution function,

$$G(r) = \frac{1}{(2\pi)^3 \rho} \int 4\pi Q^2 F(Q) \frac{\sin Qr}{Qr} \, dQ \tag{1}$$

where ρ is the atomic number density. $G(r)$ has been determined from $F(Q)$ using the program MCGR [11]. $G(r)$ is related to the partial radial distribution functions, $g_{ij}(r)$, by

$$G(r) = \sum c_i c_j b_i b_j (g_{ij}(r) - 1) \tag{2}$$

where c_i is the concentration ($= 0.5$ for CuI) and b_i the coherent neutron scattering length of species i. Information on closest approaches has also been obtained from work on crystalline [8] and molten [12] CuBr and crystalline AgBr [13]. Values were 3.5, 2.4 and 2.4 Å for I–I, I–Cu and Cu–Cu respectively at 298 K. At higher temperatures these distances were reduced slightly to allow for increased thermal motion, being 3.2, 2.2 and 2.2 Å at 713 K. Different closest-approach distances were tested but the values given were found to be most suitable.

The maximum random displacement allowed for ions was 0.1 Å in each accepted move. For each temperature the program was typically run until the fit to the data reached

equilibrium and then for a further ten hours cpu time on a DEC Alpha workstation (about 150 000 accepted moves). Ten independent configurations were collected, each separated by a further 10 hours cpu time.
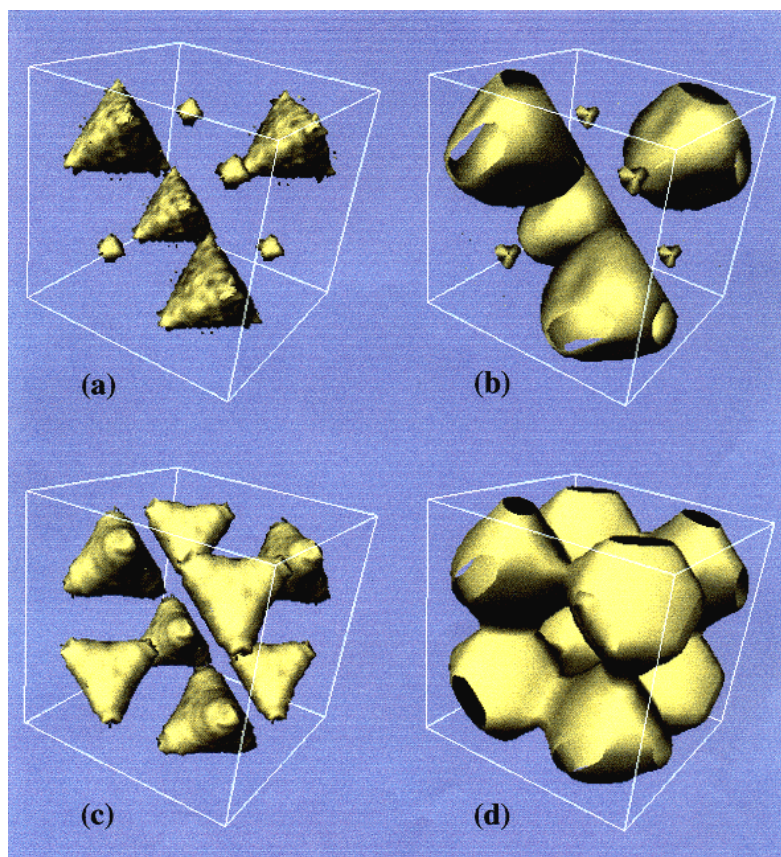

Figure 3. Constant-density isosurfaces for the average Cu^+ density distribution in CuI. The arrangement of the pictures and the temperature and density of the surface as a percentage of the maximum density in the unit cell are (a) γ-phase RMC 588 K 1.5%, (b) γ-phase MD–JM 588 K 0.5%, (c) α-phase RMC 713 K 8% and (d) α-phase MD–JM 834 K 20%.

4. Results and discussion

4.1. γ- and α-phases

The anion distributions are almost spherically symmetric. The distribution of cations in the unit cell, averaged over all 512 unit cells in all ten independent configurations for each temperature, is illustrated in figure 3. As with both MD–JM [3] and RR [1], RMC finds a tetrahedral distortion indicating large anharmonic thermal vibrations along $\langle 111 \rangle$ directions; the distortion is slightly more pronounced than in MD–JM and the density levels shown in the figure are chosen to accentuate this. In RR the distortion is modelled by replacing the highly non-spherical 8(c) (e.g. $(\frac{1}{4}, \frac{1}{4}, \frac{1}{4})$) Cu^+ 'sites' by the 32(f) (e.g. (x, x, x), $0.25 \leqslant x$) spherical sites. Each of the 32(f) sites represents one corner of the tetrahedrally distorted
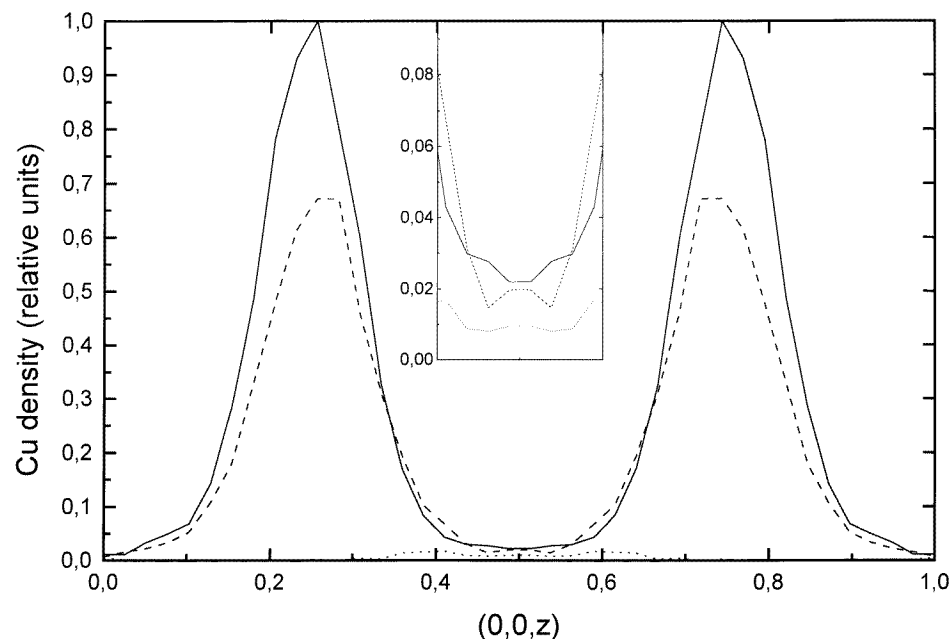
Figure 4. Average Cu^+ density distribution for α-CuI at 713 K along different paths through the unit cell (RMC model). Solid curve: between 8(c) sites along $\langle 100 \rangle$, e.g. $(\frac{1}{4}, \frac{1}{4}, \frac{1}{4}) \rightarrow (\frac{3}{4}, \frac{1}{4}, \frac{1}{4})$. Broken curve: between 32(f) sites along $\langle 100 \rangle$, e.g. $(x, x, x) \rightarrow (1 - x, x, x)$ $(x = 0.3)$. Dotted curve: between 8(c) sites along $\langle 111 \rangle$, e.g. $(\frac{1}{4}, \frac{1}{4}, \frac{1}{4}) \rightarrow (\frac{3}{4}, \frac{3}{4}, \frac{3}{4})$. The inset shows the same data on an expanded density scale.

8(c) sites and the average 32(f) site occupancy is 0.125. RR finds $x \sim 0.3$ in the α-phase [1], which is a reasonable approximation to the RMC distribution. It is impossible to make a precise comparison of the level of interstitial occupancy since the exact definition of site occupancy has to be different in all studies. However at high temperature in the γ-phase RR finds $\sim 5\%$ interstitials, RMC $\sim 6\%$ and MD–JM $\sim 2\%$.

Figure 4 shows the RMC derived density distribution in the α-phase along different directions in the unit cell. In both MD–JM and RMC the position at which the density distributions associated with separate crystallographic sites 'join' with the highest density, indicating the preferred pathway for Cu^+ diffusion, is in the centre of the 'edges' of the tetrahedrally distorted cation distribution, i.e. the pathway is directly between neighbouring 8(c) sites, e.g. $(\frac{1}{4}, \frac{1}{4}, \frac{1}{4})$ and $(\frac{3}{4}, \frac{1}{4}, \frac{1}{4})$, along $\langle 100 \rangle$. This 'join' extends along the tetrahedral edges, being only slightly lower between neighbouring 32(f) sites, e.g. $(0.3, 0.3, 0.3)$ and $(0.7, 0.3, 0.3)$. In common with MD–JM and RR, RMC finds no occupation of the octahedral site at $(\frac{1}{2}, \frac{1}{2}, \frac{1}{2})$, i.e. there is no maximum in the density distribution at this position. At the highest temperature in the α-phase there is some density (see figure 4), indicating some diffusion along $\langle 111 \rangle$ directions, but this is much lower than the $\langle 100 \rangle$ diffusion. A tetrahedron has four corners but six edges, so there are more $\langle 100 \rangle$ pathways than $\langle 111 \rangle$ pathways, and hence we estimate that less than 25% of diffusion goes through the octahedral site, the proportion decreasing as temperature decreases.

It may therefore be considered that in these terms, i.e. in terms of the average cation distribution and the preferred diffusion direction, all three studies (RMC, MD–JM and RR) produce remarkably consistent results.

$G(r)$ from the RMC model at 713 K is shown in figure 5, in comparison to MD–JM.
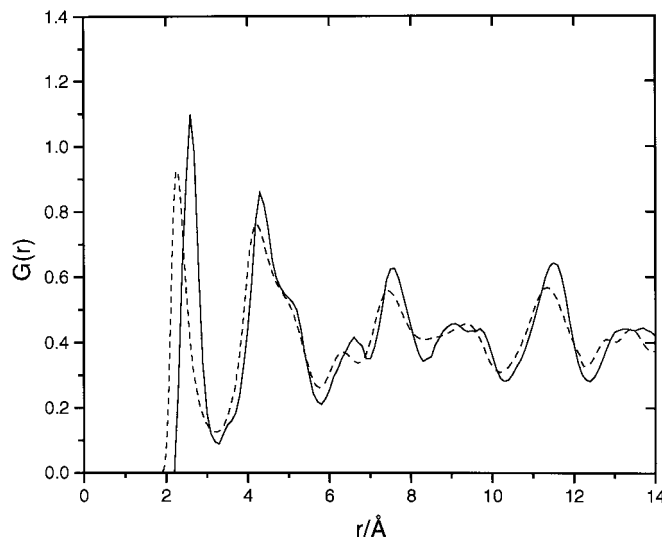
Figure 5. Total radial distribution function, $G(r)$, for α-CuI from RMC modelling at 713 K (solid) and MD–JM simulation at 834 K (dash).

It can be seen immediately that the first peak, corresponding to the nearest-neighbour Cu–I separation, occurs at significantly lower r in MD–JM than in RMC. The same result is found in all three phases. The RMC results are consistent with what would be expected from the lattice parameters and the average crystal structure, which is that the peak occurs at $\sim$2.6 Å, the distance increasing slightly as temperature increases and the material expands. Given that the average Cu^+ and I^- positions in the unit cell are very similar for MD–JM and RMC (as described above), and hence the distances between the average positions are also similar, it is necessary to explain how the peak positions in $G(r)$ can be so different.

A peak in $G(r)$ represents the distribution of separations of *individual* ions and their *individual* neighbours. If the motions of all ions are independent then the peak in $G(r)$ will be at the same position as expected from the average crystal structure. However if there are correlations between the motions of individual neighbouring ions then the positions may be different. Consider that the unit cell for the γ-phase illustrated in figure 1(a) represents a single unit cell within the material, i.e. the spheres represent individual atoms rather than atomic sites. If, when the I^- ion in the bottom right-hand corner of the cell happens to have moved from its site towards the cube centre, there is an increased probability that the neighbouring Cu^+ ion 'occupies' the 32(f) site closest to that I^- ion, then the first peak in $g_{CuI}(r)$ will be shifted to lower r relative to a situation in which there is no increased probability.

The partial radial distributions, $g_{ij}(r)$, are shown in figure 6 for all temperatures in the RMC study. $g_{CuI}(r)$ changes effectively continuously through all phases, i.e. the Cu^+ environment within the I^- sub-lattice is similar despite the change in the sub-lattice in the β-phase. In fact this is not surprising since the β-phase anion packing is only slightly different from the γ- and α-phases. The most significant change occurs in $g_{CuCu}(r)$ where a distinct peak grows at low r, $\sim$2.4 Å, as the ionic conductivity increases. This distance represents the separation between 'lattice' and 'interstitial' sites in the γ-phase, i.e. $(\frac{1}{4}, \frac{1}{4}, \frac{1}{4}) \rightarrow (\frac{3}{4}, \frac{1}{4}, \frac{1}{4})$. Such a peak does not occur in the MD results (figure 6). An equivalent peak has been observed in similar experimental studies of CuBr [8], AgBr [13]
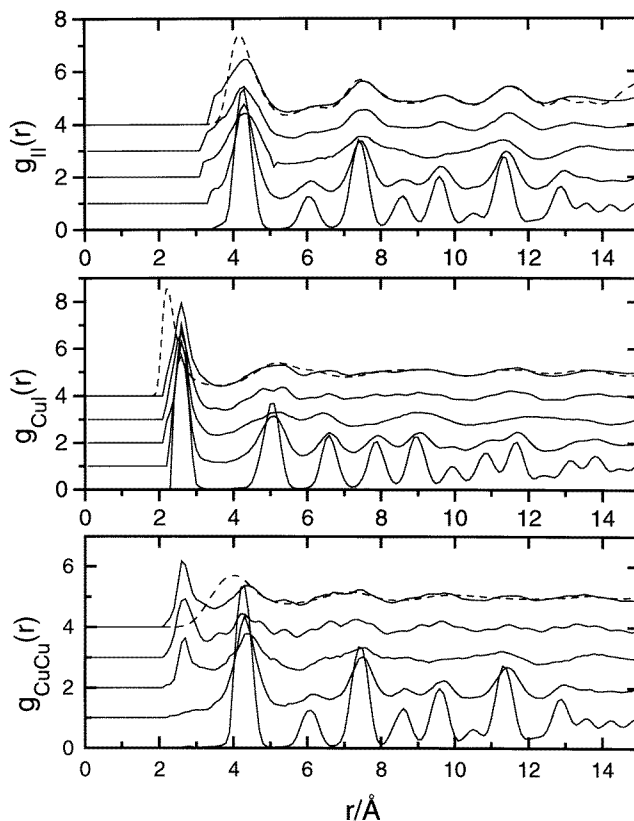
Figure 6. Partial radial distribution functions, $g_{ij}(r)$, from RMC modelling for CuI at (in ascending order) 298 and 588 K in the γ-phase, 663 K in the β-phase and 698 and 713 K in the α-phase. Consecutive curves are shifted by 1.0 for clarity. The dashed curves show the results from MD–JM at 834 K in the α-phase.

and AgI [14]. An anomalous x-ray scattering study of molten CuBr [15] and an isotopic substitution study of Ag/Cu chalcogenide glasses [16] have also shown evidence of a similar low-r peak. In order to test whether this peak is 'real', or is somehow an artefact of RMC modelling, we have applied a constraint to the average Cu–Cu coordination, i.e. to the integral of $g_{CuCu}(r)$, between 2 and 3.5 Å. As we force the coordination to decrease, i.e. the peak to grow smaller, then the fit to the data becomes rapidly worse, in particular in the region of the broad diffuse scattering peak at ~ 1 Å^{-1}. It is not possible to adequately fit the experimental data with a significantly reduced first peak in $g_{CuCu}(r)$, so the feature must be real. It is interesting to note that the peak occurs closer to the 2.46 Å distance between nearest-neighbour 32(f) sites than to the 3.07 Å distance between 8(c) sites.

The correlation with the ~ 1 Å^{-1} diffuse scattering peak is easily explained. If $g_{CuCu}(r)$ were zero below 3.5 Å then it would mean that Cu$^+$ did not simultaneously occupy neighbouring 8(c)/32(f) sites, so diffusion could only occur if all Cu$^+$ moved coherently. This is not likely, so some intensity at low r in $g_{CuCu}(r)$ is necessary; even in MD $g_{CuCu}(r)$ extends down to ~ 2.5 Å. If there is random occupation of the 8(c)/32(f) sites in the α-phase then the Cu–Cu coordination should be 3, i.e. the $g_{CuCu}(r)$ peak should be rather intense. The value from the RMC model is 2.25 at 713 K, which indicates some local correlations

between the occupation of neighbouring cation sites; i.e. if a site is occupied then the probability of its neighbouring sites being occupied is slightly reduced. Random occupation (e.g. 'ideal' α-phase), or zero probability of occupation of neighbouring sites (e.g. 'ideal' γ-phase), produce no 100 Bragg peak for the structure. Other occupation probabilities will produce broad diffuse scattering around the same position in Q, i.e. ~ 1 Å^{-1}, exactly as is observed. From the width of the diffuse scattering it is clear that the correlation only extends over one to two unit cells. Changing the Cu$^+$ distribution to decrease the height of the $g_{CuCu}(r)$ peak will therefore alter the diffuse scattering at low Q, as we have found.

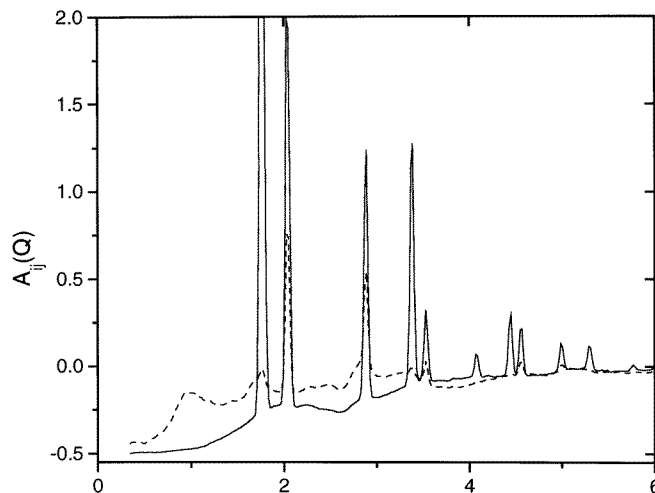**Figure 7.** Partial structure factors, $A_{ij}(Q)$, for CuI at 713 K in the α-phase. Solid: $A_{II}(Q)$. Dash: $A_{CuCu}(Q)$.

In figure 7 we show the partial structure factors, $A_{ij}(Q)$, for the α-phase at 713 K. These have not been calculated by Fourier transform of $g_{ij}(r)$ since this would result in a broadening of all features due to the finite size of the RMC simulation (see e.g. [13]); they have been calculated directly from the atomic positions in the configuration, using a new method to approximate the diffuse scattering [17]. It can be seen that the 1 Å^{-1} diffuse scattering peak definitely occurs in $A_{CuCu}(Q)$, and not in $A_{II}(Q)$ (or in fact in $A_{CuI}(Q)$), thus confirming the analysis above that relates it to cation correlations.

We now need to explain why the peak in $g_{CuCu}(r)$ does not occur in the MD–JM results, even though the simulation reproduces the experimental diffusion rate. In order to produce a low-r peak in $g_{CuCu}(r)$ in the MD–JM simulation it would be necessary to reduce the effective charge on Cu$^+$ (a value of 0.81 was used), since Coulomb repulsion is the dominant interaction between Cu$^+$ at short distances. However, in order to maintain charge neutrality it would be necessary to also reduce the effective charge on I$^-$. This would result in a significant change in the energy of optic modes, but this energy has been used as one of the criteria for determining the potential. Effectively in MD–JM the diffusion has been maintained at the correct (high) level by keeping a high effective charge but reducing the Cu–I repulsive part of the potential, i.e. by making Cu$^+$ 'small'. This then clearly leads to the local correlation between Cu and I observed in the low r value of the first peak in $g_{CuI}(r)$. To produce a low-r peak in $g_{CuCu}(r)$ without this distortion requires an additional effective attraction between Cu$^+$ ions that will alter $g_{CuCu}(r)$ but not $g_{CuI}(r)$; this is not possible with only two-body interactions. We have previously proposed, on the basis of MD

studies of the complete set of Cu halides [4], that three-body terms related to the polarization of the large I^- ions by the small Cu^+ ions would be appropriate. This is further supported by the results shown here.

In the case of 'normal' crystalline materials at low temperatures, where diffusion is effectively zero, it is usually obvious how to define 'sites' within the crystal structure. However for fast ionic conductors at high temperatures, where diffusion may be comparable to that in the corresponding liquids, some care is needed to ensure that a mathematically possible definition also makes some physical sense. In a recent molecular dynamics study of α-CuI Ihata and Okazaki [18] (MD–IO) have interpreted the Cu^+ distribution by polyhedron analysis. They consider cations to be 'in' a particular site if they are inside the volume (polyhedron) assigned to that site. The unit cell is then divided into eight tetrahedra surrounding the tetrahedral sites and six octahedra surrounding the octahedral sites, and all polyhedra are joined by triangular faces. The cation density distribution from MD–IO [18] is in fact very similar to the MD–JM results [3] (which is unsurprising since the potential used is very similar) and the present RMC results. However the polyhedron method of analysis produces the result that about 35% of cations are in octahedral sites, which is considered to be consistent with EXAFS results [19] which assign 30% to octahedral sites. Ihata and Okazaki [18] also suggest that, because the centre of mass of the Cu^+ which are 'in' octahedral sites is located at the centre of the octahedron (which of course it must be by symmetry), then these cations may be considered to be 'at' the octahedral site, despite the fact that most of them are in fact located close to the faces of the octahedron and far from the centre. This type of 'mathematical' assignment makes no physical sense. It is clear from the results of RR, MD–JM, RMC and MD–IO that Cu^+ undergo large anharmonic thermal vibrations about the tetrahedral sites and along $\langle 111 \rangle$ directions. These vibrations are so large that the cations often penetrate into the volume (octahedron) surrounding the octahedral site, but most often they return to their original tetrahedral site or diffuse to a neighbouring tetrahedral site along a $\langle 100 \rangle$ direction. Only rarely, and at the highest temperatures, do Cu^+ pass close to the centre of the octahedron (see e.g. figure 4). The octahedral site is always at a minimum in the cation density distribution, and the cation energy here is high, so it is more realistic to categorize the site as one that is 'avoided' rather than one that is occupied.

A short comment can be made in relation to EXAFS analysis. EXAFS effectively measures the short-range instantaneous local order around a particular atomic species, and so the results should be quite comparable to the total scattering data measured here. In the case of Cu EXAFS from CuI [19] the quantity measured is related to $g_{CuI}(r) + g_{CuCu}(r)$. However the analysis has considered that only $g_{CuI}(r)$ will contribute at short distances, whereas we have shown quite clearly that $g_{CuCu}(r)$ also has a peak at about the same position as that in $g_{CuI}(r)$. This will obviously have some distorting effect on the conclusions of the EXAFS data analysis.

4.2. β-phase

The discussion above related to the partial radial distribution functions and the origin of the diffuse scattering peak at low Q also applies to the β-phase. In fact the radial distribution functions change systematically between γ-, β- and α-phases (figure 6) indicating that there is no discontinuity in short-range order despite the change in symmetry of the long-range order. The structure factor in the β-phase also shows a broad diffuse scattering peak at low Q, which is almost centred at the same position as the 100 Bragg peak at 0.87 Å^{-1}. The presence of this Bragg peak is one of the main reasons that Keen and Hull [1, 10]

chose the $P\bar{3}m1$ space group to refine the crystal structure rather than $P\bar{6}_3mc$ (Wurtzite structure) which had been used previously [20, 21]. This choice implies some preferential correlation of the occupation of B and C sites (or equivalently A and D—see figure 1(b) for site nomenclature). Each B site has three neighbouring C sites with an average occupation of 0.5, so the average Cu–Cu coordination should be 1.5 for random occupation. The low-r peak in $g_{CuCu}(r)$ from RMC gives a coordination of 1.95, implying preferential correlation in agreement with Keen and Hull; the RMC result would imply a site occupation of about 0.65, slightly smaller than their value of 0.75.

In contrast to the γ- and α-phases, the average density in the unit cell for the β-phase shows interesting differences in detail between RMC, RR and MD–JM. The higher density levels (i.e. the majority of ions) in RMC and MD–JM are actually closer than for the γ- and α-phases, but at low densities the distribution has a different shape. In figure 8 it can be seen that the MD–JM cation distribution has a definite threefold symmetry about the a axis (vertical in the figure), but this is missing in both RMC β-I and β-II results which seem to have only one of the three 'lobes'. The anion distribution also shows some asymmetry, being elongated along the a axis (it is slightly elongated in MD–JM as well). As might be expected, given the different starting configurations, RMC β-I has a higher Cu$^+$ density between the tetrahedral sites and β-II a higher density at the tetrahedral sites. Both results are equally consistent with the available data.

The RMC Cu$^+$ distribution must distort away from spherical symmetry around the A, B, C and D sites because the first peak in $g_{CuCu}(r)$ is at a shorter distance than the distance between B and C sites (or A and D). This is entirely consistent with the tetrahedral distortion in the γ- and α-phases. However RR used an isotropic distribution for the β-phase since it was found that an anisotropic distribution was not required to fit the data (hence if an anisotropic distribution were used the results might not be physically meaningful). In the γ- and α-phases the tetrahedral distortion is taken care of by replacing the anisotropic 8(c) sites by isotropic 32(f) sites. The RR treatment of the β-phase therefore seems to be inconsistent with the expected similarities in local order in the different phases, and also with the fact that the β-phase has a high conductivity. The RMC results suggest that the local structure in the β-phase is distorted in a way that is incompatible with the long-range symmetry, which may explain why this structure is not particularly stable. In principle it would be possible to perform RMC modelling using both the high-resolution RR data and the high-systematic-accuracy RMC data, and hence to obtain a consistent solution for the structure, but a program for doing this is not yet available.

5. Conclusions

We have shown that there is a high degree of consistency between RR, MD–JM and RMC results for the average cation distribution in the unit cell for all three phases of CuI, though there are some differences in detail. In the γ- and α-phases Cu$^+$ undergo large anharmonic thermal vibrations about the tetrahedral sites and along $\langle 111 \rangle$ directions but diffuse to neighbouring tetrahedral sites along $\langle 100 \rangle$ directions. The octahedral site is not 'occupied'. In the β-phase there is a local structural distortion which is incompatible with the long-range symmetry of the crystal structure.

The local cation correlations show significant differences between MD–JM and RMC (RR provides no direct information on local correlations). The MD–JM results are in fact inconsistent with the experimentally determined total radial distribution functions, independent of RMC modelling. The RMC results show clearly that there is a short-distance peak in $g_{CuCu}(r)$ in the fast-ion-conducting phases, implying correlations between
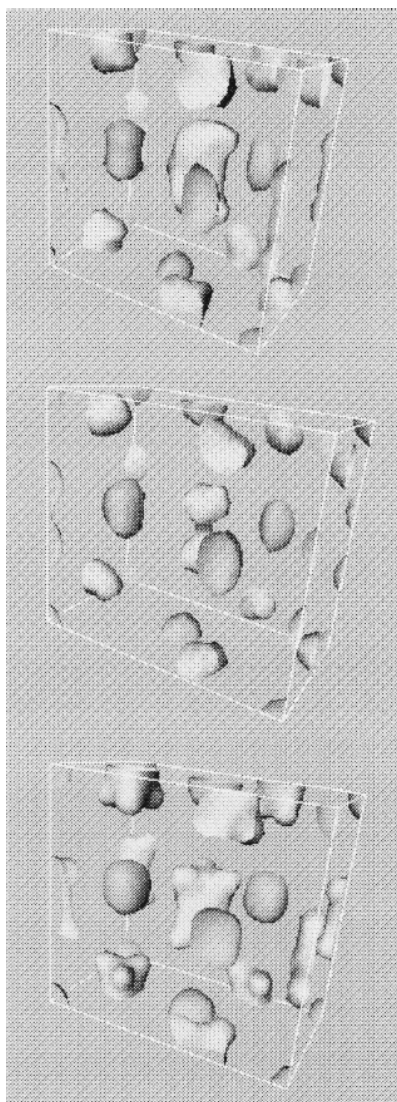
Figure 8. Constant-density isosurfaces for the average Cu^+ (lighter) and I^- (darker) density distributions in β-CuI. The density chosen is 20% of the maximum density in the unit cell. Top: RMC β-I model at 663 K. Centre: RMC β-II model at 663 K. Bottom: MD–JM simulation at 665 K.

the occupation of neighbouring cation sites. Such a peak has been observed before in AgBr, AgI and CuBr, but for the first time we have here been able to demonstrate that this peak is clearly related to the observation of a broad diffuse scattering peak at $Q \sim 1$ Å^{-1} in the experimental data, and hence cannot be an artefact of the RMC modelling procedure. To reproduce such a feature in an MD simulation almost certainly requires the introduction of three-body terms in the interatomic potentials.

Acknowledgment

References

[1] Keen D A and Hull S 1995 *J. Phys.: Condens. Matter* **7** 5793
[2] Zheng-Johansson J X M, Ebbsjo I and McGreevy R L 1995 *Solid State Ion.* **82** 115
[3] Zheng-Johansson J X M and McGreevy R L 1996 *Solid State Ion.* **83** 35
[4] McGreevy R L and Zheng-Johansson J X M *Solid State Ion.* **95** 215
[5] Dejus R, Sköld K and Graneli B 1980 *Solid State Ion.* **1** 327
[6] Zheng-Johansson J X M, Sköld K and Jørgensen J-E 1992 *Solid State Ion.* **50** 247
[7] Azaroff L V 1961 *J. Appl. Phys.* **32** 1658
[8] Nield V M, Keen D A, Hayes W and McGreevy R L 1994 *Physica* B **202** 159
[9] McGreevy R L 1997 *Computer Modelling in Inorganic Crystallography* ed R A Catlow (London: Academic)
     p 151
[10] Keen D A and Hull S 1994 *J. Phys.: Condens. Matter* **6** 1637
[11] Pusztai L and McGreevy R L 1997 *Physica* B **234–236** 357
     Pusztai L and McGreevy R L 1997 *Phys. Scr.* submitted
[12] Allen D and Howe R A 1992 *J. Phys.: Condens. Matter* **4** 6029
[13] Nield V M, Keen D A, Hayes W and McGreevy R L 1992 *J. Phys.: Condens. Matter* **4** 6703
[14] Nield V M, Keen D A, Hayes W and McGreevy R L 1993 *Solid State Ion.* **66** 247
[15] Waseda Y, Saito M, Park C and Omote K 1997 *Sci. Rep. RITU* A **43** 195
[16] Salmon P and Liu J 1996 *J. Phys.: Condens. Matter* **205–207** 172
[17] Mellergård B A and McGreevy R L 1997 *Phys. Scr.* submitted
[18] Ihata K and Okazaki H 1997 *J. Phys.: Condens. Matter* **9** 1477
[19] Boyce J B, Hayes T M and Mikkelsen J C Jr 1981 *Phys. Rev.* B **23** 2876
[20] Miyake S, Hoshino S and Takenaka T 1952 *J. Phys. Soc. Japan* **7** 19
[21] Krug J and Sieg L 1952 *Z. Naturf.* **7** 369